

UNCLASSIFIED

AD 406 286

DEFENSE DOCUMENTATION CENTER

FOR

SCIENTIFIC AND TECHNICAL INFORMATION

CAMERON STATION, ALEXANDRIA, VIRGINIA



UNCLASSIFIED

NOTICE: When government or other drawings, specifications or other data are used for any purpose other than in connection with a definitely related government procurement operation, the U. S. Government thereby incurs no responsibility, nor any obligation whatsoever; and the fact that the Government may have formulated, furnished, or in any way supplied the said drawings, specifications, or other data is not to be regarded by implication or otherwise as in any manner licensing the holder or any other person or corporation, or conveying any rights or permission to manufacture, use or sell any patented invention that may in any way be related thereto.

406 286

406286

BPSN: 2(3-3145)-61081

63.3-6

RESEARCH INVESTIGATION
OF
MAGNETIC AND ELECTRIC FORCES
FOR ROTATING SHAFT SUSPENSION

Technical Progress Report
March 1963 through May 1963

Contract No. AF 33(657)-8352

Research Laboratories for the Engineering Sciences

University of Virginia

Charlottesville



Report No. EMI-4454-114-63U

June 1963

The work covered by this report was accomplished under Air Force contract, but this report is being published and distributed prior to Air Force review. The publication of this report, therefore, does not constitute approval by the Air Force of the findings and conclusions herein. It is published for the exchange and stimulation of ideas.

BPSN: 2(3-3145)-61081

RESEARCH INVESTIGATION OF MAGNETIC AND ELECTRIC FORCES
FOR ROTATING SHAFT SUSPENSION

Technical Progress Report
March 1963 through May 1963

Contract No. AF 33(657)-8352

Submitted by:
B. J. Gilpin

RESEARCH LABORATORIES FOR THE ENGINEERING SCIENCES
UNIVERSITY OF VIRGINIA
CHARLOTTESVILLE, VIRGINIA

Report No. EMI-4454-114-63U
June 1963

Copy No. 14

BPSN: 2(3-3145)-61081

ABSTRACT

The radially passive bearing system is found to have an excessively flexible shaft. The system is rotated with an air turbine and dynamic load tests show no coupling between a pure torque load and the rigid body modes of the shaft. The completed mechanical system for the radially active bearing is given and the modified current drivers are described. The continuing analysis and experimental effort to achieve damping in the resonant magnetic bearing system are given.

TABLE OF CONTENTS

SECTION I	INTRODUCTION.	1
SECTION II	PASSIVE RADIAL BEARING SYSTEM	
	G. A. Smith	2
SECTION III	D. C. MAGNET SYSTEM	
	C. L. Epley and G. T. Theisz, Jr.	7
	A. Requirements	7
	B. Support Stator	7
	C. Support Rotor	7
	D. Support Rotor and Stator Characteristics . .	7
	E. Position Sensor	10
	F. Motor and Shaft	12
	G. Control Amplifiers	12
	H. Axial Confinement	12
	I. Future	12
SECTION IV	RESONANT MAGNET SUPPORT	
	D. F. Nieman	15

LIST OF ILLUSTRATIONS

<u>Figure</u>		
1	DYNAMIC RESPONSE OF SHAFT	4
2	EDDY CURRENT LOAD.	6
3	SUPPORT STATOR.	8
4	SUPPORT ROTOR	9
5	SENSOR	11
6	RADIALLY ACTIVE SUPPORT CONTROL AMPLIFIER	13
7	OPPOSED RESONATED ELECTROMAGNETS S-PLANE ROOT LOCI.	17
8a	BLOCK DIAGRAM IMPLEMENTATION OF DIFFERENTIAL EQUATION	20
8b	TRANSFORMED BLOCK DIAGRAM IN ABSENCE OF EXTERNAL DISTURBANCES	20
9	ROOT LOCUS PLOT-EFFECT OF INSTRUMENTING A SIMPLE DIFFERENTIATOR.	20
10	BLOCK DIAGRAM INITIAL ACTIVE DAMPING TRIAL	22
11	COMPOSITE GAIN AND PHASE VS FREQUENCY PRELIMINARY RESONANT MAGNETIC SUPPORT COMPENSATION	23
12	BLOCK DIAGRAM-RESONANT ELECTROMAGNET PAIR VELOCITY SENSING	24

SECTION I
INTRODUCTION

When the passive radial bearing system is operated with a horizontal shaft, there is sag in the bearings until the restoring force from the bearings equals the total weight of the rotating member. This sag was equal to the normal air gap for the Air Force motor. The last quarterly report gave the attempt to by-pass this problem by operating the system with a vertical shaft. This mode of operation gave rise to problems which overshadowed the sag problem and the system was returned to its horizontal shaft arrangement.

This quarterly report describes: 1) the attempted operation of the Air Force motor with the stator of the motor lowered to compensate for the sag and with auxiliary mechanical constraints having a 5-mil radial clearance; 2) the lack of success; 3) the operation with an air turbine; and 4) the dynamic behavior of the shaft with intermittent loads.

The mechanical structure of the radially active, d.c. magnet, system has been completed. Included in this report are the final drawings and a description of several of the components. The phase splitter, which allows one position sensor to control the opposite pairs of support poles, is shown on the circuit of the control amplifiers.

The analysis of the magnetic resonant system is continued in this report. Based on the linearized equations for the system, a root locus plot is derived. Also, the value of applied voltage necessary to give critical damping is determined. The location of the actual operating conditions graphically points out the inadequacy of the intrinsic damping. The effect of electrical compensation is also presented in a root locus plot. Also described in this report is the continuing experimental effort to achieve damping by active electrical means.

Included here is a description of a magnetic bearing that recently was made commercially available by the Cambridge Thermionic Corporation.

SECTION II PASSIVE RADIAL BEARING SYSTEM

G. A. Smith

After the system was returned to the horizontal shaft configuration, an attempt was made to determine the effect of servomagnet and servo-armature misalignment on radial damping. The only result was qualitative. When the complete system is as perfectly aligned as practical, the radial damping is less than that obtained from a less critical alignment procedure. It has not been possible to determine how to "misalign" the system for best results as far as radial damping is concerned.

In order to attempt to operate the Air Force motor with the shaft horizontal, it was necessary to lower the stator of the motor to compensate for the inherent sag of the shaft in the bearings. (The motor air gap is only 8 mils.) The outer stator ring was machined so that it could be lowered as much as 7 mils. Also, mechanical restraints which limit radial shaft movement to ± 5 mils were installed for protection of the motor armature during run-up through the trouble speeds. Finally, a variable voltage 400 cps, 3 phase, power supply system was assembled to drive the Air Force motor.

With low voltage applied, the motor was run through the trouble speeds up to a speed of about 3200 rpm. However, contrary to all previous experience with the small fan motor, the running was not smooth--even above the trouble speeds--and full line voltage could not be successfully applied to the motor.

While the procedures for dynamically balancing a shaft was being studied, the stator of the motor and the radial mechanical restraints were removed and an air turbine was installed. The air turbine provides a way of rotating the shaft without introducing the radial forces present in an energized motor. When the system was rotated by means of the air turbine, the operation was again smooth above 2500 rpm.

Up to this point in the development, the observation of smooth running had been the basis for the inference that above 2500 rpm, the

radial shaft motion ceased and the shaft was running as a straight rod. However, a closer look was taken of the operating system using a strobe light operating slightly off the running speed of the shaft. It showed that although the operation is smooth, the shaft is actually bowed and there is considerable (about 10 mils) runout at the center of the shaft at 3000 rpm. Further, as the speed is increased, the bow (and runout) of the shaft increased.

By using proximity displacement gages at the center and end of the shaft, the curves shown in Figure 1 were obtained. These curves show: 1) the large excursion of the end of the shaft as it passes through the rigid body rotational frequency; 2) the large peak in the excursion of the center of the shaft at the rigid body translational frequency; and 3) the increasing deflection of both the center and the end of the shaft with increasing speed above 3000 rpm. By observing the relative phase of these excursions, it was established that the shaft was bending and running but not flexing or bent.

Further displacement measurements made at the bearing armatures show no radial motion up to about 900 rpm, but in the smooth running range above 2500 rpm, the bearing armatures are actually undergoing several thousandths runout. This fact should be kept in mind, for it is a characteristic that distinguishes these noncontacting "confining" systems from their conventional hard bearing counterparts.

At present it is not possible to test the bearings because the flexible shaft and the 8-mil air gap of the motor are restricting the operation to very low speeds. It will take considerable machining to allow a shaft to be installed that is four times as stiff as the present shaft and even this increase will not allow testing at rated speed. It is clear that the apparent performance of these bearings depends to a large extent on other factors of the system and on the job they are asked to do. For example, this bearing system has performed quite satisfactorily when the small fan motor was on the shaft. But with the 1-hp motor, the performance was entirely unsatisfactory. These considerations serve

BPSN: 2(3-3145)-61081

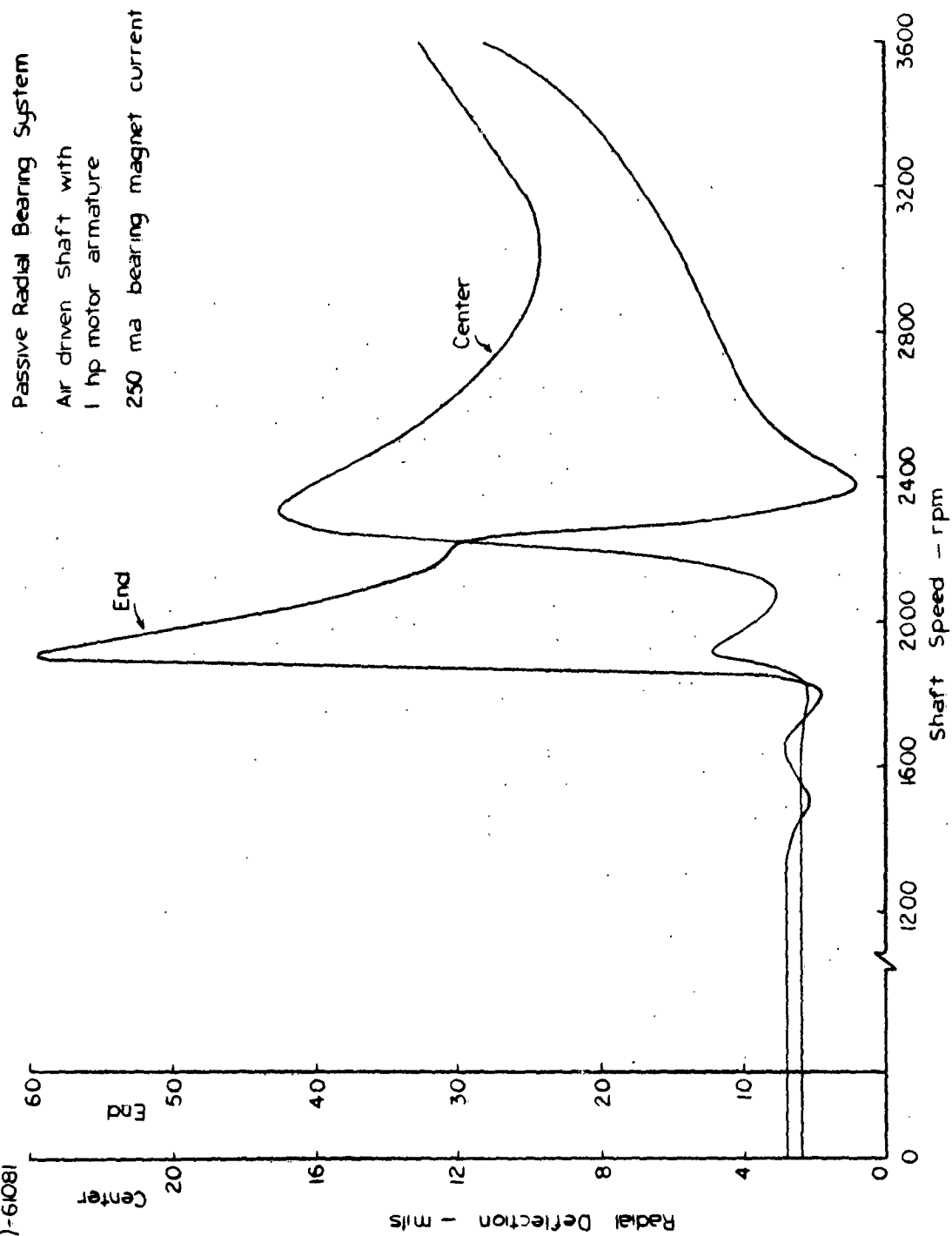


FIGURE 1
DYNAMIC RESPONSE OF SHAFT

4454-97

point up the problem of accurately determining the capability of the bearings independently of other system characteristics.

While an approach to this latter problem is being sought, other characteristics of the bearing system are being studied. Eddy current loads have been installed at each end of the shaft. Essentially each load consists of four E-shaped electromagnets. By means of a fixed steel plate, the flux from the electromagnets is directed through an aluminum plate that rotates with the shaft, Figure 2. While driving the shaft at 3400 rpm with the air turbine, the current in the eddy current load magnets was varied sinusoidally, triangularly and as a square wave over a frequency range from 0 to 50 cps. This range was chosen so that the rigid body modes would be excited if there is interaction between the application of the load and the bearing system. (Note: The rigid body modes of 1900 and 2300 rpm correspond to 31.7 and 38.4 cps.) The load was applied long enough to lower the shaft speed from 3400 to 3200 rpm.

No adverse effects were observed even when the load was pulsed near the rigid body frequencies. It is concluded that a pure torque load does not excite the normal modes of the shaft.

A start has been made toward measuring the static torques associated with the passive bearings. These measurements will continue since they help determine the stiffness of the shaft on which the bearings are mounted. (After the shaft was found to be bending under the centrifugal load, a careful measurement showed that the cocking action of the bearings caused a small deflection of the shaft independently of any rotational forces.) If it could be determined that the bearing characteristics are unaltered by rotation, a set of static characteristics would completely describe the bearing.

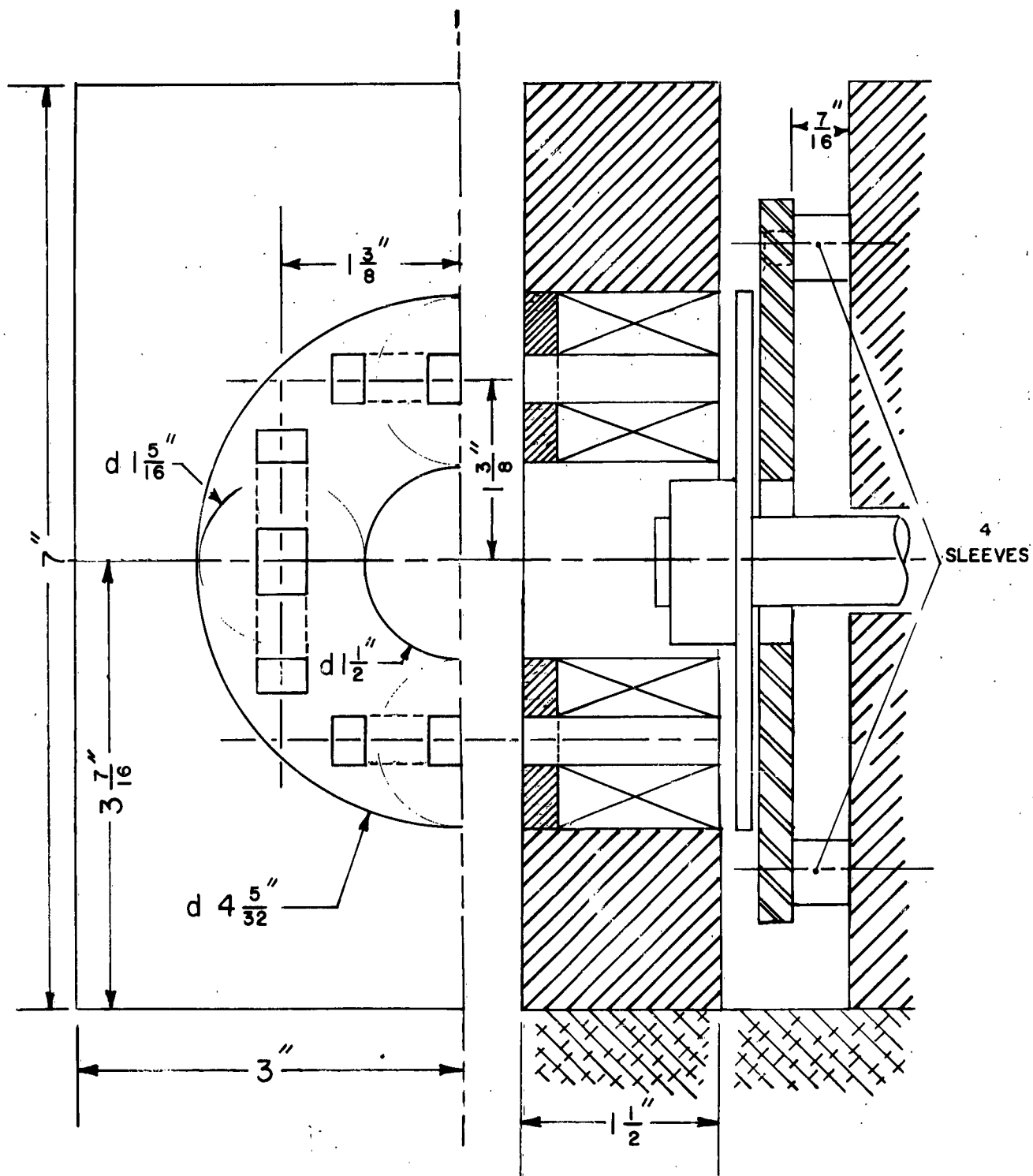


FIGURE 2
EDDY CURRENT LOAD

SECTION III
D. C. MAGNET SYSTEM
C. L. Epley and G. F. Theisz, Jr.

A. Requirements

The design of the "final model" has several fixed requirements which are: 1) fit 4" bronze cradle as used with the passive bearing system; 2) use 8-pole d.c. motor punchings obtained; and 3) be able to use fan motor used in other systems as well as Air Force motor. With these boundaries as well as the information obtained from the "breadboard model", the system was designed.

B. Support Stator

Each support stator is composed of 50, 8-pole, 14 milli-inch, AISI M-19 transformer steel laminations. The 8 poles are wound in four groups of two, so that for each of the four directions of force, there is a north-south pole pair. One winding of each north-south pole pair is a d.c. bias winding and the other is a control amplifier winding. The winding per pole pair consists of 350 turns of A. W. G. number 26 wire, Figure 3.

C. Support Rotor

The support rotor is constructed of 0.75" of 7 milli-inch Armco Tran-cor T electrical steel. This material was chosen to simplify construction and because it is a better electrical steel than the stator, Figure 4.

D. Support Rotor and Stator Characteristics

When the rotor is centered in the air gap, each pair of poles exert 25 pounds of force on the rotor. The net force on the rotor for a 10% current change is 5.9 pounds. At present, the control amplifier gain is set so that a 1 milli-inch displacement causes a 33% current change per pole pair. Thus, the net force on the rotor is 21 pounds for a rotor

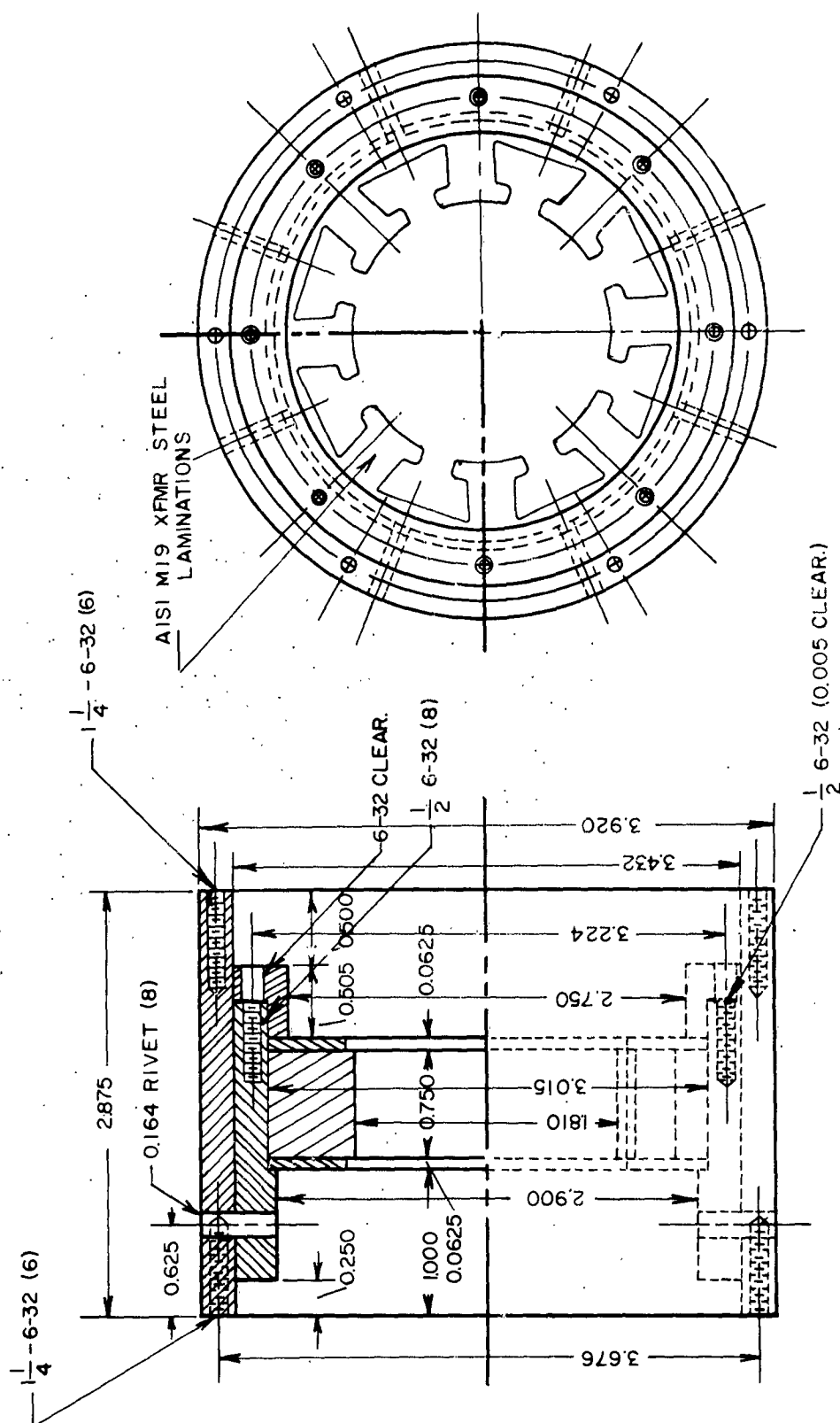


FIGURE 3
SUPPORT STATOR

BPSN-2(3-3145)-61081

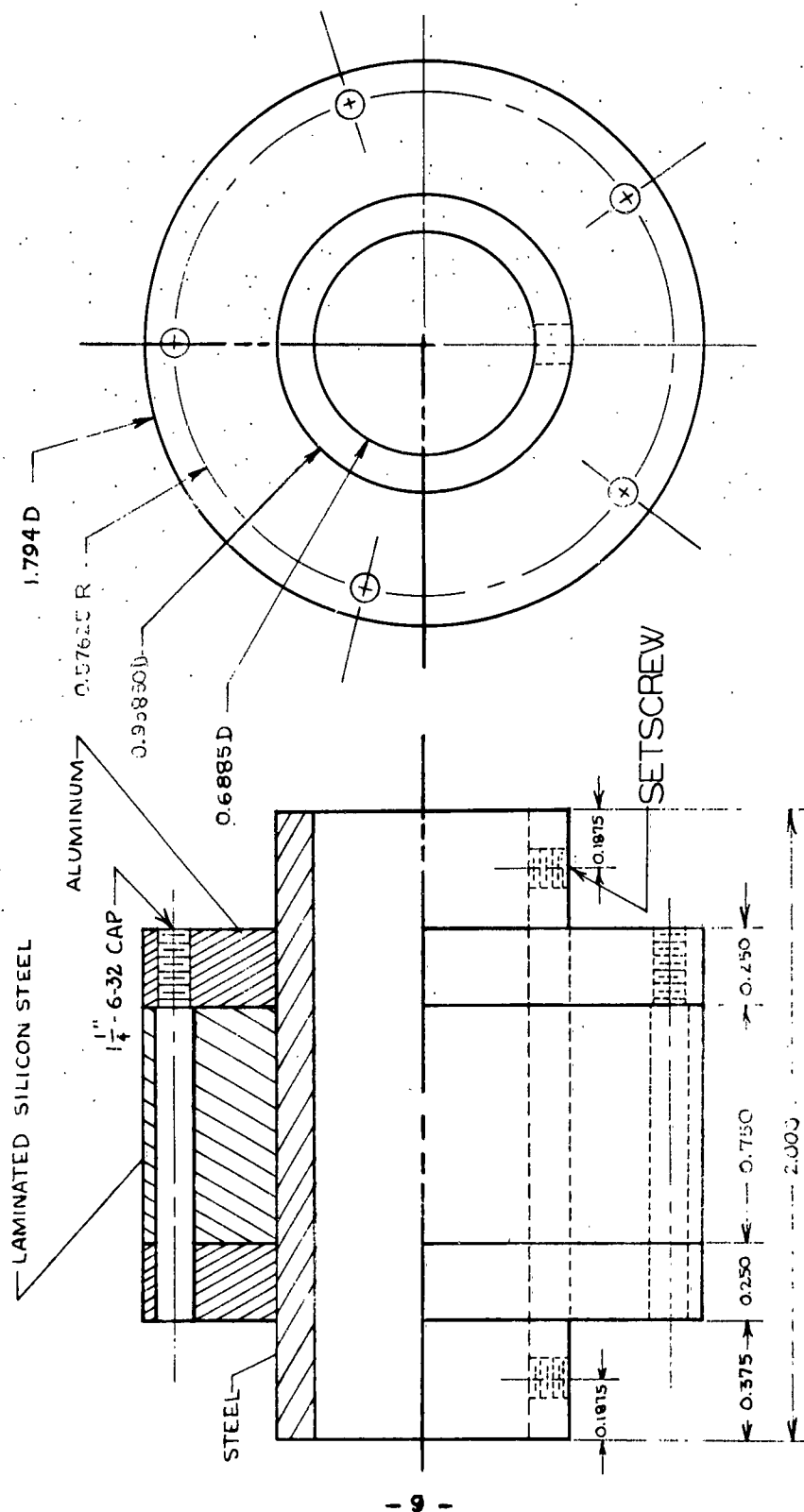


FIGURE 4
SUPPORT ROTOR

displacement of 1 milli-inch. (All force values are calculated.)

The electrical steel used in the rotor and stator have the best magnetic characteristics that could be obtained and used with a minimum of fabrication effort. The magnetic properties are probably equal to those found in the best motors commercially available. It is felt that lower quality magnetic materials could be used; however, this idea should be checked.

The model uses an 8 milli-inch radial air gap and as expected, sag of the supported member will occur as a result of gravity. The sag may be removed however, by adjustment of the operating point of the control amplifiers.

E. Position Sensor

1. Stator

The stator element for the position sensor is shown in Figure 5. The outer piece is grounded. Each pair of the inner pieces, 90° apart, form the plates of a capacitor in a 455-kcps tuned circuit.

2. Rotor

The rotor element is a commutator taken from a d. c. motor and forms the movable plate of a variable capacitor. A d. c. motor commutator was used as the second plate of the capacitor because the mica insulates the copper bars from each other and the shaft. Thus, the x direction position sensor does not cause a voltage to appear on the y direction sensor as would occur with a solid conducting rotor.

3. Rotor-Stator Characteristics

As the supported rotor moves, the capacitance changes, shifting the frequency of the tuned circuit so that the magnitude of the 455-kcps voltage applied to the control amplifier changes in accordance with position of the supported rotor.

A radial air gap of 10 milli-inches is used here, compared to 8 milli-inches for the support portion, to prevent contact of the two

FIGURE 5
SENSOR

plates of the capacitor even if contact occurs at the support poles. The capacitance per sensor is 35.8 μfd when the rotor is in center position.

F. Motor and Shaft

The motor now being used is the same small fan motor used in the other systems. Any motor with a stator outside diameter of less than 3.920 inches (the size of the bronze cradle used with the passive bearing system) may be installed.

The shaft is solid stainless steel and is obtained as a stocked item centerless ground to a diameter of 0.6875 inches.

The elements of the system may be so arranged as to accept loads or motors anywhere on the length.

G. Control Amplifiers

The circuit for the control amplifiers is shown in Figure 6. These amplifiers are now in the process of being modified to allow more control of the system. A complete discussion of their characteristics will appear in the next quarterly report.

H. Axial Confinement

There is no axial unbalance force for this type of support system: in fact, for axial displacements, on the order of $1/2$ the support rotor length ($3/8$ inches), there is a large restoring force. For small displacements, there is almost no restoring force so that some type of confinement will have to be used. This confinement can be obtained by static fields or active fields. (For instance, an active system like that used for axial confinement in the passive radial system.)

I. Future

As soon as the improvements are completed on the control amplifiers, (about two weeks), the effort will be directed toward stable support of this system. The improvements are directed toward simplifying stability

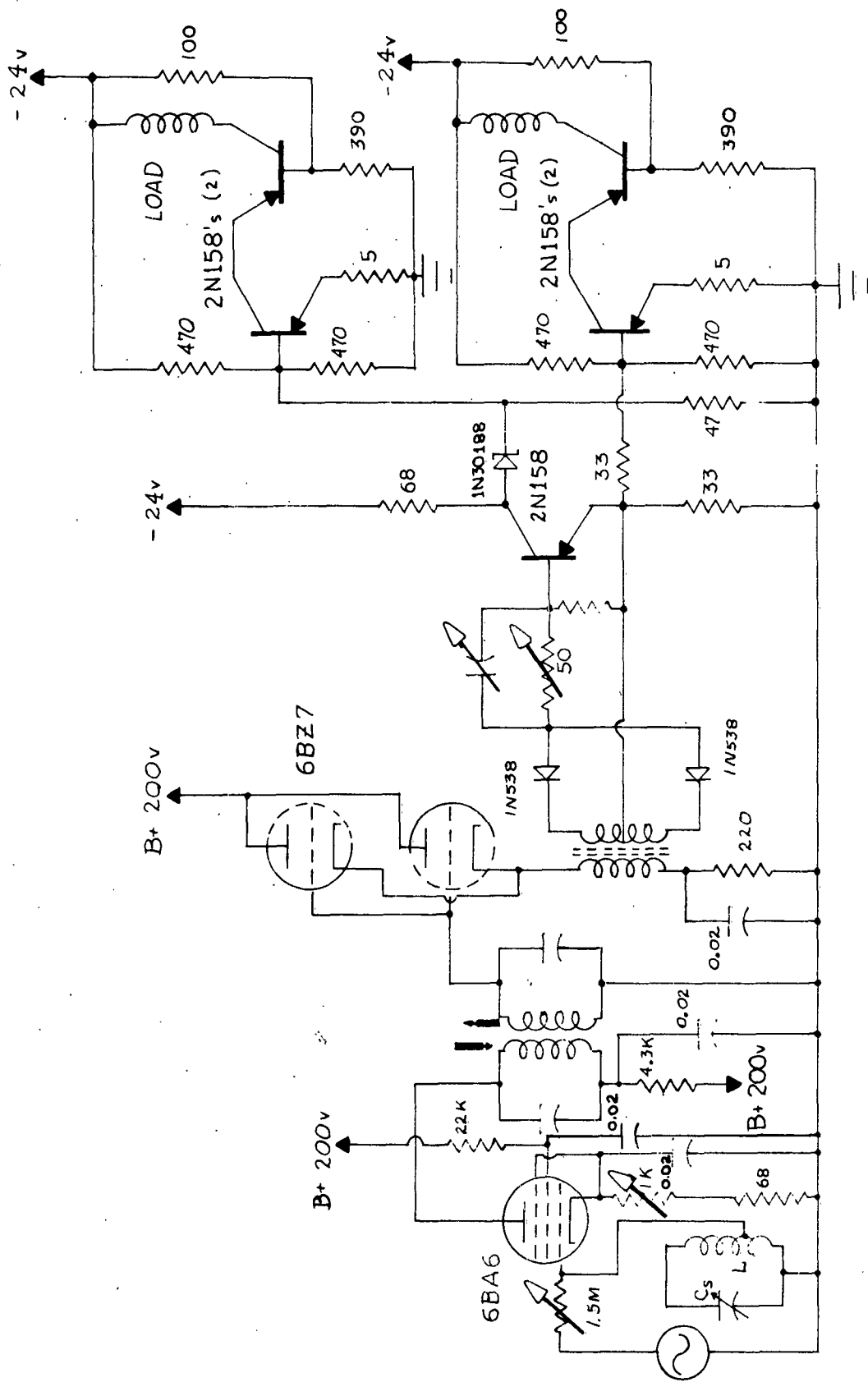


FIGURE 6
RADIALLY ACTIVE SUPPORT
CONTROL AMPLIFIER

problems by isolating the position control from the a.c. gain control in the servo loop. Following support, measurements can be made on the stiffness and other characteristics of the system.

SECTION IV RESONANT MAGNET SUPPORT

D. F. Nieman

A previously derived¹ relation describing the dynamic behavior of a free armature working as a force summing member between two opposed resonated electromagnets is given below:

$$m\ddot{x} + \left[\frac{b L_0 E}{X_{\text{net}}^2 + r^2} \right]^2 r \dot{x} + \left[\frac{b L_0 E}{X_{\text{net}}^2 + r^2} \right]^2 \Omega X_{\text{net}} x = Q(x, t) ,$$

a detailed form of the usual equation:

$$m\ddot{x} + D\dot{x} + Kx = Q(x, t) ,$$

where $Q(x, t)$ is an externally applied force. Under appropriate assumptions, this relation transforms to:

$$ms^2 x(s) + Ds x(s) + Kx(s) = Q(s) ,$$

which yields the transfer function:

$$\frac{x(s)}{Q(s)} = \frac{\frac{1}{m}}{\left(s + \frac{D}{2m} + j \sqrt{\frac{K}{m} - \left(\frac{D}{2m} \right)^2} \right) \left(s + \frac{D}{2m} - j \sqrt{\frac{K}{m} - \left(\frac{D}{2m} \right)^2} \right)}$$

Both quantities D and K contain the "gain-factor" $[b L_0 E / X_n^2 + r^2]^2$ which may be considered a parameter.

Information as to the mechanical response of the armature may be obtained from a root locus plot of the above transfer function, X/Q , as the gain factor varies from zero to infinity. This parametric variation physically may correspond to raising the excitation voltage E , for example. Such a

¹ Quarterly Progress Report, Report No. EMI-4454-109-62U; November 1962, p. 41.

s-plane plot is shown in Figure 7. It is instructive to locate several operating points of the 2-D test rig, with only intrinsic damping, relative to this root locus plot. System numerical values from a previous report² will be employed. For simplicity and also to approach the case of an armature shaft combination magnetically confined and noncontacting, it will be assumed that the shaft assembly of Figure 5 in reference 2 undergoes radial translation so that the two magnetic bearings work in consort. From the reference cited, it follows that:³

$$\begin{aligned} K &= 2 (90 \cdot E^2) \text{ Newtons/meter} \\ D &= 2 (5.5 \cdot 10^{-3} E^2) \text{ Newtons/meter/sec} \\ m &= 2 \text{ Kg} . \end{aligned}$$

The relation for the roots of the denominator becomes:

$$s = -E^2 \left[2.75 \cdot 10^{-3} \pm j \sqrt{\frac{90}{E^2} - 7.6 \cdot 10^{-6}} \right] .$$

Critical damping occurs when:

$$\frac{90}{E^2} = 7.6 \cdot 10^{-6} \quad \text{or} \quad E = 3440 \text{ volts,}$$

which corresponds to,

$$s_c = -247 \cdot 10^3 \text{ radians/sec} .$$

By comparison, to date, the maximum employable value of E has been 40 volts, for which D and K have been previously calculated.⁴

² Quarterly Progress Report, Report No. EMI-4454-111-63U; March 1963, p. 18.

³ Ibid., pp. 12, 22.

⁴ Ibid.

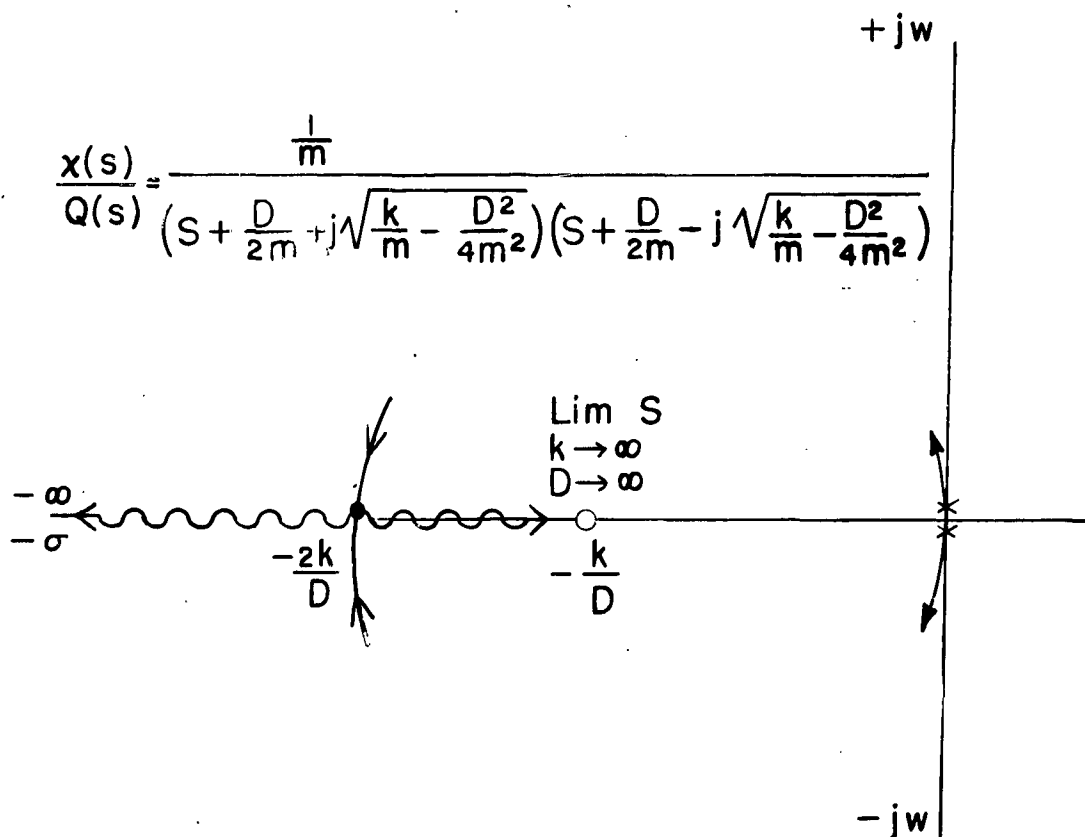


FIGURE 7

OPPOSED RESONATED ELECTROMAGNETS
S-PLANE ROOT LOCI

For such conditions, the corresponding values of s are:

$$s = -4.4 \pm j 378 \text{ rad/sec.}$$

From this it is clear that intrinsic damping at a feasible operating point is quite inadequate.

Historically, at this point in the study, information reached this laboratory of a marketed device known as the "Magcentric" bearing--a product of Cambridge Thermonics Corporation. Subsequently, this bearing was demonstrated at this laboratory. The device uses nominally concentric rings of colinear magnetic dipoles producing inner and outer toroidal magnetic fields of like direction. Such means is employed at each end of the shaft to produce radial restoring forces. The attendant axial upsetting force is balanced by magnetic forces on a central disk. These axial magnetic forces providing constraint are derived from opposing resonated electromagnets. Assuming mechanical damping is not involved, even when operated in a vacuum, the analysis in this report is applicable. Configurations operated at this laboratory have not been free of mechanical constraint. Accordingly, there was high interest in the "Magcentric" bearing with regard to stability. Pertinent comments about one version of this system follow:

1. Radial stiffness is such that the 18-gram rotor will possibly encounter mechanical interference at an acceleration of two times gravity (2g);
2. The axial stiffness, the active or controlled direction, is such that mechanical interference is likely at about 4 g acceleration when adjusted as per manufacturer's procedure;
3. Normal, or manufacturer's preferred, operation of the bearing is where magnet current lags the driving voltage by nearly 90° , and one or both waveforms are distorted. These conditions result in stable confinement at rather low stiffness. If the driving voltage frequency is now lowered, it is required (for stability) that the bearing housing be mounted on a compliance, in one case polyurethane foam;

4. When the shaft is rotating, this compliance is also required. This is evidenced by periodic mechanical interference when the bearing housing is clamped rigidly to the table;
5. The driving frequency is 13 Kc with resonance occurring at 10 Kc.

Tentatively, it is concluded that the magcentric bearing may be operated stably due to various intrinsic loss processes in conjunction with very low stiffness.

To illustrate the possible effects of active damping; i. e., that obtained from additional control circuitry, the equation describing the dynamic behavior may be represented as in Figure 8(a). Further manipulation of the linear system and substitution of various circuit values results in Figure 8(b) where it is assumed that no external disturbance exists. The root locus diagram is that of Figure 7, wherein it may be seen that if D could be increased without attendant increase in K , more favorable solutions might be attained. Of course, a differentiation followed by magnet current modification, i. e., inverse rate feedback, of necessity must be band limited at the high frequency end. Figure 9 shows the root locus, in solid lines, for such a simple differentiator which is represented by the zero at $-K/D$ and a pole to the left of this zero. The desired effect being to increase the damping for a particular gain. The inevitable poles at higher frequencies due to eddy currents, hysteresis, filtering out of the driver frequency, etc., modify the root locus as suggested by the broken line characteristic. The important point here is that the resonant magnetic support system may be investigated stability-wise like other systems.

In the experimental effort to electrically achieve active damping, prior circuitry⁵ is not presently in use. Large switching signals derived from the current waveform in one magnet were required. During development of a Schmitt Trigger circuit for this purpose, it was decided to change

⁵ Quarterly Progress Report, Report No. EMI-4454-109-62U; December 1962, p. 36.

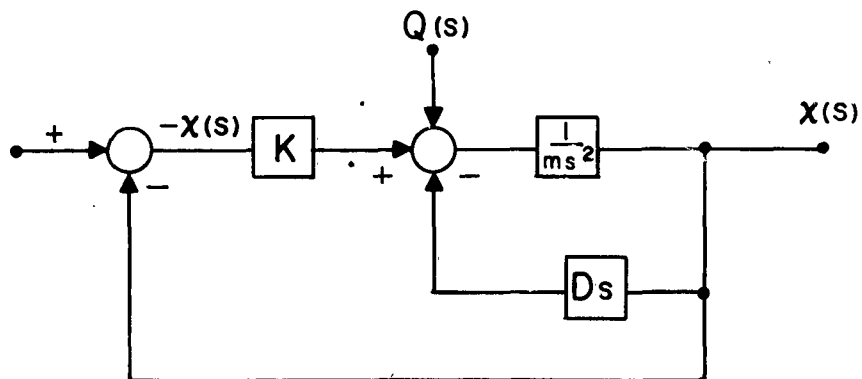


FIGURE 8a

BLOCK DIAGRAM IMPLEMENTATION OF DIFFERENTIAL EQUATION

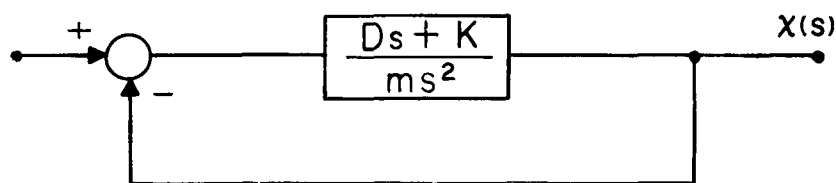


FIGURE 8b

TRANSFORMED BLOCK DIAGRAM IN
ABSENCE OF EXTERNAL DISTURBANCES

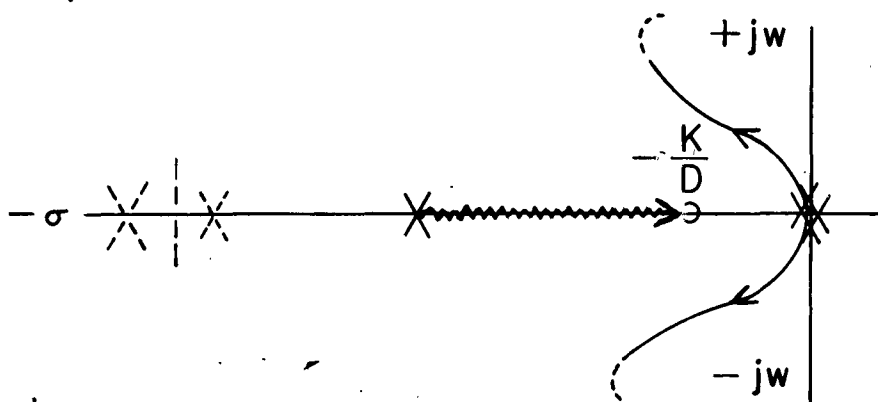


FIGURE 9

ROOT LOCUS PLOT—EFFECT OF
INSTRUMENTING A SIMPLE DIFFERENTIATOR

the method. The setup employed during this period was as shown in block diagram form in Figure 10.

The output of the bistable multivibrator after low pass filtering is a d. c. voltage proportional to the phase angle between the driving voltage and the current in one magnet. Differentiation of this voltage and application to an electromagnet exerting a force colinear with the armature motion was to effect damping. Noise problems were encountered particularly with 60-cycle and its harmonics. Reference to Figure 11 shows the necessity for elimination or reduction of extraneous voltages.

In spite of the extraneous signal problems for weak spring like forces and small electrical damping signal, qualitatively, it may be said that active damping was effected using the 1-D test rig. Efforts to employ more damping resulted in large average current in the damper electromagnet (due to noise) which produced an unbalanced force causing the armature to displace excessively. Accordingly, a new physical embodiment of the approach in Figure 10 was begun. The details are shown in Figure 12. This approach uses the phase difference between the currents in opposing magnets for position information. The compensation initially will be that shown in Figure 11.

It is hoped that careful attention to layout plus any benefits arising from this new difference method will give a better demonstration of active damping.

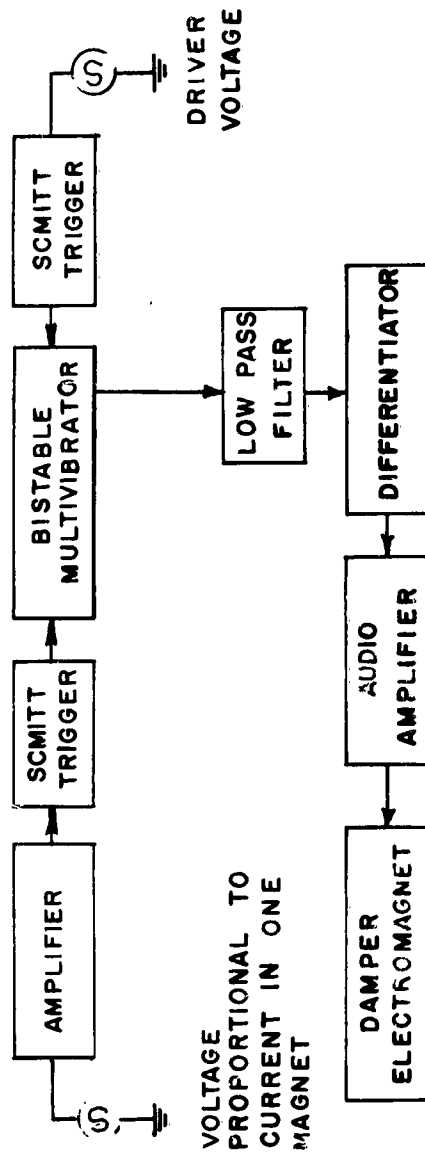


FIGURE 10
BLOCK DIAGRAM INITIAL ACTIVE DAMPING TRIAL

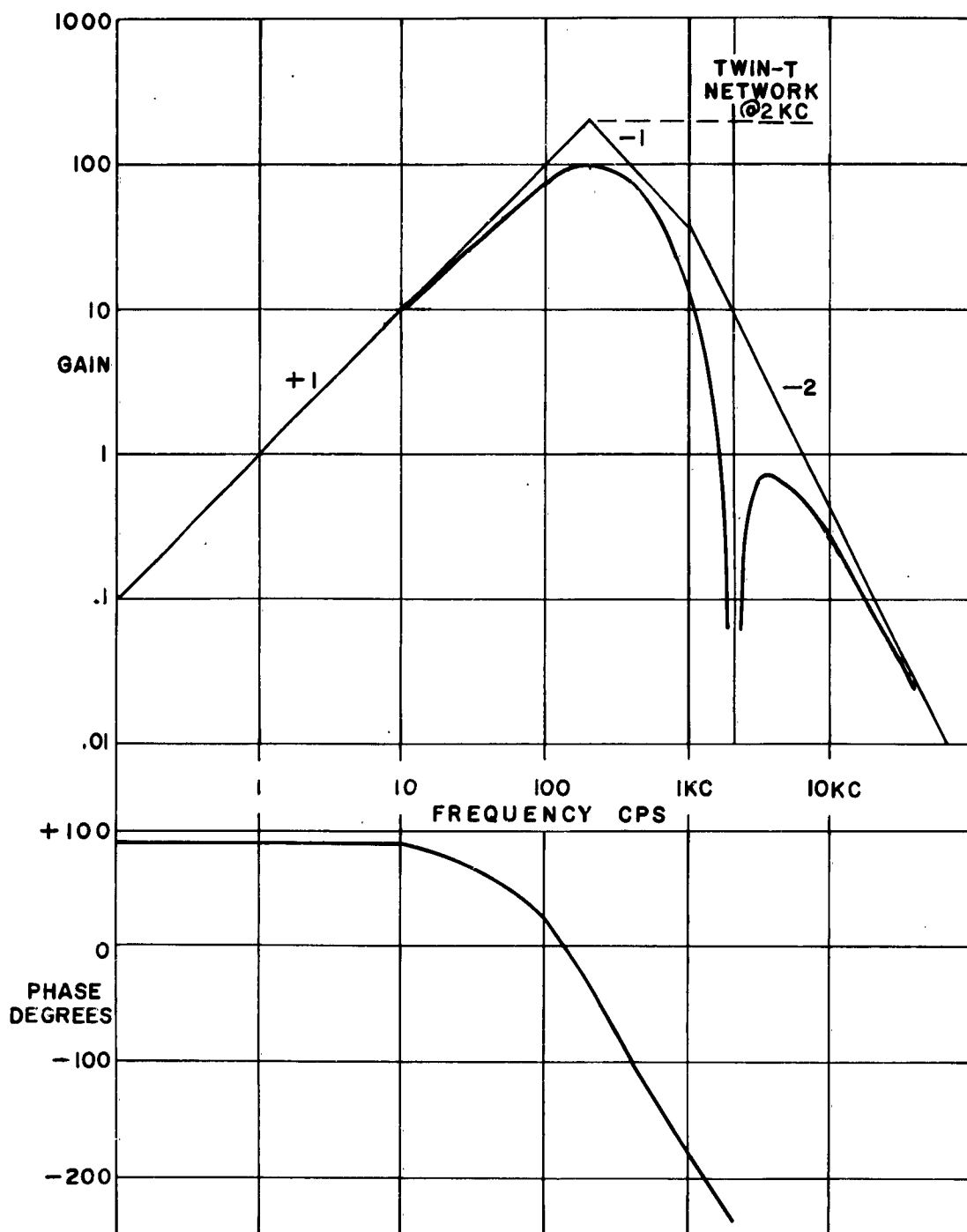


FIGURE II
COMPOSITE GAIN AND PHASE VS. FREQUENCY
PRELIMINARY RESONANT MAGNETIC SUPPORT COMPENSATION

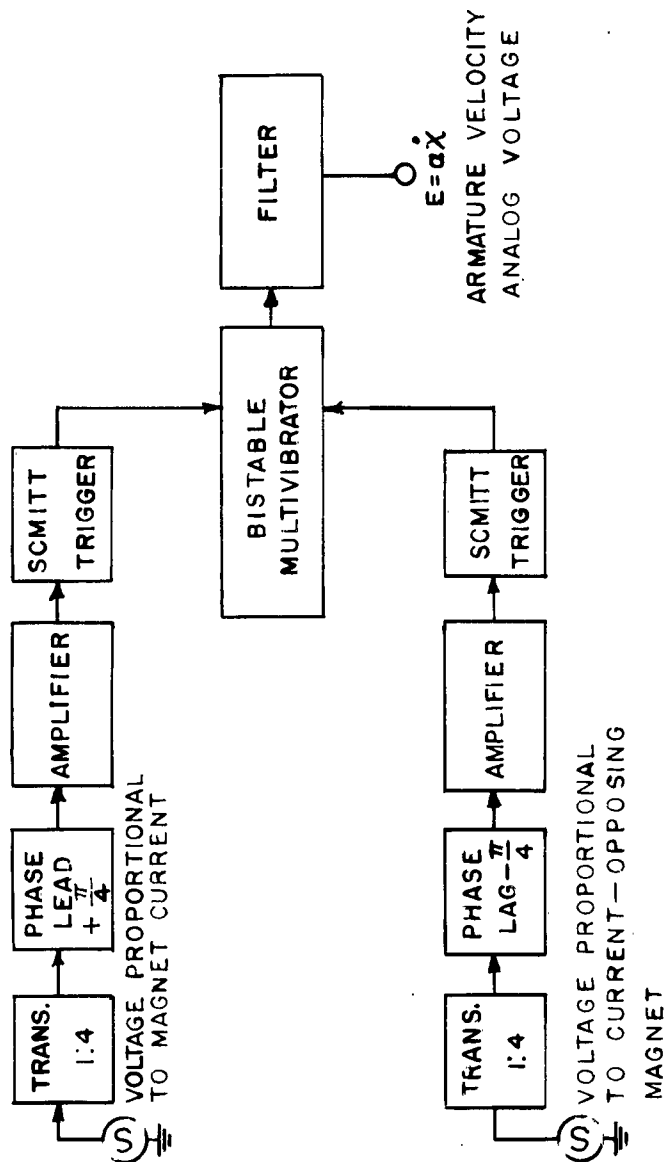


FIGURE 12
BLOCK DIAGRAM-RESONANT ELECTROMAGNET PAIR
VELOCITY SENSING

DISTRIBUTION LIST

Copy No.

1 - 11	Aeronautical Systems Division ATTN: ASRMFP-3 Wright-Patterson Air Force Base, Ohio
11 - 30	ASTIA Arlington Hall Station Arlington 12, Virginia
31	National Aeronautics and Space Administration Lewis Research Center 21000 Brook Park Road Cleveland 35, Ohio
32 - 34	B. J. Gilpin
35	A. R. Kuhlthau
36	E. C. Stevenson
37	J. W. Moore
38	E. S. McVey
39	H. S. Landes
40 - 45	RLES Files